Flow normal to a short cylinder with hemispherical ends

G. J. Sheard,[1,2] M. C. Thompson,[1] and K. Hourigan[2]
[1]*Fluids Laboratory for Aeronautical and Industrial Research (FLAIR), Department of Mechanical and Aerospace Engineering, Monash University, Victoria 3800, Australia*
[2]*Division of Biological Engineering, Faculty of Engineering, Monash University, Victoria 3800, Australia*

(Received 2 January 2008; accepted 29 February 2008; published online 7 April 2008)

The flow normal to a cylinder with hemispherical ends is computed using a spectral-element/Fourier method. With variation in the ratio of cylinder length to diameter, this body varies smoothly from a sphere to a straight circular cylinder, providing insight into the relationship between body topology and wake dynamics. This letter displays the wake structure for a range of cylinder lengths up to a Reynolds number of 300 and considers the wake alignment and symmetry at length ratios approaching a spherical body. A time-invariant wake consistent with that behind a sphere is found to preferentially align with a symmetry plane bisecting the major axis of short cylinders, whereas the periodic "hairpin" wake aligns with the minor axis; thus the hairpin vortices shed from alternate sides of the cylinder, just as with Kármán vortex shedding from a circular cylinder. The plane of symmetry is found to break via a supercritical transition at a Reynolds number of 350 ± 2. © *2008 American Institute of Physics*. [DOI: 10.1063/1.2899782]

The transitions which occur in the wakes of bluff bodies such as the sphere and the straight circular cylinder have been the subject of a vast number of studies in recent decades.[1–3] These bodies undergo a well-known and distinct set of transitions with increasing Reynolds number, with bifurcations due to both time-dependent and three-dimensional instability modes occurring, respectively, at Reynolds numbers $\mathrm{Re}=46$ and $\mathrm{Re}\approx 190$ for cylinders,[1,4,5] and at $\mathrm{Re}=211$ and $\mathrm{Re}\approx 270$ for spheres.[3,6,7]

Mittal[8] numerically studied the unsteady nonaxisymmetric wakes behind both spheres and spheroids and found that at over the range of $350\lesssim \mathrm{Re}\lesssim 375\pm 10$, the wake of a sphere loses the planar symmetry it preserved through both the regular nonaxisymmetric and Hopf bifurcations. No subsequent efforts have yet further refined this transition Reynolds number, and the irregularity of the wake beyond this transition has left open the question as to whether the transition might be hysteretic (subcritical) or continuous (supercritical).[9,10]

Studies have attempted to relate the nature and order of these transitions to geometric parameters defining the body. Thick rings (tori) were used to study bodies of revolution other than a sphere,[11] and slender rings were used to investigate circular cylinders without end effects.[12] The full range of ring aspect ratios was later completely characterized numerically.[13,14] Straight circular cylinders of finite length have been widely studied due to their importance both in aero- and hydrodynamic engineering applications, as well as in understanding the influence of end effects on the otherwise parallel shedding behind the cylinder span.[15–17] These studies observe marked differences in the transition Reynolds numbers and wake characteristics as the cylinder aspect ratios (ratios of length to diameter) approach $O(1)$.

Recent experimental studies have considered finite-length cylinders with hemispherical ends,[18,19] chosen deliberately to recover a sphere for a unit aspect ratio, as an alternative geometry for systematically investigating the relationship between geometry and wake bifurcation scenario. These studies measured Strouhal–Reynolds number profiles and estimated the critical Reynolds numbers for the onset of unsteady flow and their relationship with aspect ratio. No visualization of the wakes behind cylinders with hemispherical ends has yet been published.

This letter investigates the flow past cylinders with hemispherical ends with aspect ratios up to 5. Firstly, the numerical treatment of the geometry is described. Subsequently, visualization of the vortical structure of the wakes at a range of aspect ratios is presented. Finally, a short cylinder is used to further investigate the transitions which develop behind a sphere, with consideration paid to the preferred orientations of the regular and periodic planar-symmetric wakes, as well as a detailed characterization of the transition leading to the loss of planar symmetry.

A schematic representation of the system under investigation and the coordinate system being employed is given in Fig. 1. A Reynolds number is defined $\mathrm{Re}=Ud/\nu$, where U is the free-stream velocity, d is the cylinder diameter, and ν the fluid kinematic viscosity. This study considers $\mathrm{Re}\lesssim 300$, a range which encompasses the transitions to unsteady and three-dimensional wake flow for both a sphere and a straight circular cylinder. Taking the cylinder length as L allows a length ratio definition $\mathrm{LR}=L/d$.

The cylinder with hemispherical ends differs from the aforementioned axisymmetric bodies in that the symmetry axis of the body is aligned *normal* to the direction of flow, instead of parallel to the direction of flow. This has implications on the numerical modeling of this problem, as discussed in the next section.

This study employs the same spectral-element/Fourier code that has previously been employed to study the wakes behind spheres and rings.[9,14] The numerical formulation follows closely to the algorithm employed by Tomboulides and

1070-6631/2008/20(4)/041701/4/$23.00

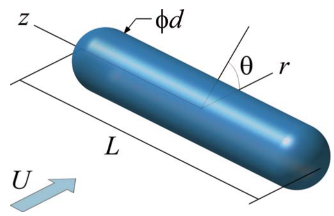

FIG. 1. (Color online) The coordinate system relative to a cylinder with hemispherical ends. Flow is normal to the z-axis.

Orszag,[7] and described neatly by Blackburn and Sherwin.[20] A nodal spectral-element method is used to discretize the velocity and pressure fields on the z-r plane, and a Fourier expansion resolves azimuthal variations in the flow variables. Elements are concentrated in the vicinity of the cylinder surface to resolve regions of high spatial gradients such as boundary-layer flows. A mesh employed is shown in Fig. 2.

For time integration a third-order Adams–Bashforth scheme explicitly advances the nonlinear advection terms of the incompressible Navier–Stokes equations, continuity is enforced by projecting the velocity field onto a divergence-free space during solution of the pressure term, and the viscous term is computed implicitly using a theta-modified Crank–Nicolson scheme.

The development of the wake normal to axis of symmetry requires a large number of Fourier planes to properly resolve the wake. A test case was established for a sphere (LR=1) at Re=300, with simulations conducted at a range of element polynomial degrees (N) and numbers of Fourier planes (P=64 and 128). Eventually 128 Fourier planes and elements of degree of 11 were chosen, producing an accuracy of better than 1% for both time-averaged drag and Strouhal frequency calculations. This accuracy was maintained in further tests for Reynolds numbers Re$\leqslant$300.

A Reynolds number Re=300 exceeds the critical Reynolds numbers for unsteady and three-dimensional flow behind both spheres and straight circular cylinders, and therefore provides a useful baseline at which to investigate the effect of aspect ratio variation on the wakes. Included in Fig. 3 are isosurface plots showing the wakes behind cylinders

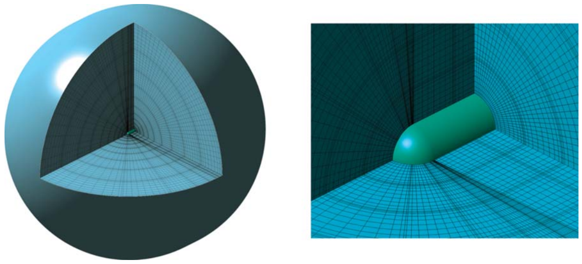

FIG. 2. (Color online) Cutaway views of the computational domain, revealing the mesh and the surface of the cylinder. Left: The left vertical and horizontal cutaway surfaces show the spectral-element mesh occupying the z-r plane, and the right vertical cutaway surface exposes the Fourier planes employed to discretize the flow in the azimuthal direction. Right: Detail of the mesh in the vicinity of the cylinder. The cylinder has LR=5, and the domain extends 30d from the cylinder.

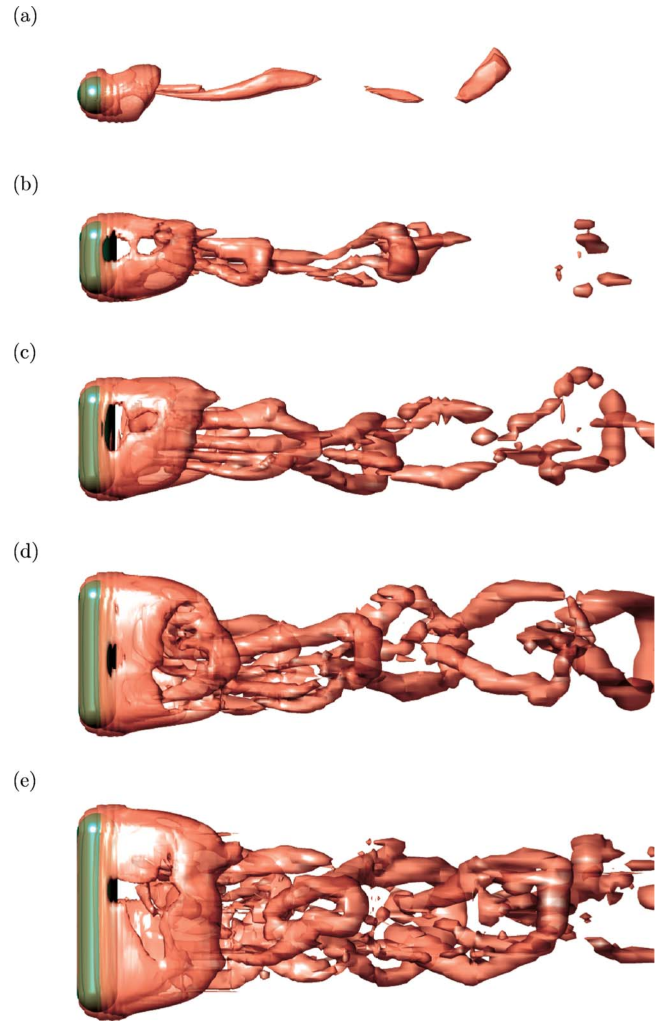

FIG. 3. (Color online) Plots of the vortical structure of the wakes behind cylinders with hemispherical ends at Re=300. Isosurfaces of the eigenvalue proposed by Jeong and Hussain (Ref. 21) are plotted to reveal vortices in the flow. Flow is left to right, and translucent isosurfaces reveal the cylinder at the left of each frame. Parts (a)–(e) show length ratios LR=1, 2, 3, 4, and 5, respectively.

with length ratios up to LR=5 at Re=300. It can be seen that at smaller length ratios the wakes are not symmetrical about the cylinder midspan. This asymmetry is associated with the Strouhal frequency of the spanwise component of force acting on the cylinder and is less prominent with increasing LR.

Coinciding with the development of spanwise symmetry is the development of vortices resembling Kármán vortices in the vicinity of the cylinder midspan and within approximately 1d-3d downstream. Evidence of this is shown by solid vertical bands in the isosurface plots in Figs. 3(d) and 3(e).

A very short cylinder (length ratio LR=1.04) was considered to develop an understanding of the relationship between azimuthal asymmetry of a nearly spherical body and the resulting wake symmetries.

The familiar steady nonaxisymmetric wake comprising a counter-rotating pair of vortices extending far downstream was computed at Re=250. Orthogonal views of an isosurface plot of this solution are shown in Fig. 4. These views verify

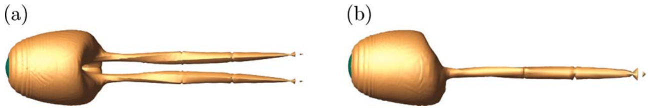

FIG. 4. (Color online) The steady wake computed at Re=250 for a cylinder with LR=1.04. Orthogonal top (a) and side (b) views are shown. Isosurfaces and flow direction are as per Fig. 3. The dimples in the vortical tails are plotting artifacts at element interfaces.

the presence of planar symmetry (the plane is aligned with the major axis of the body) and illustrate the close similarity to the wake behind a sphere.[7]

Here the recirculation bubble shifts in the direction of the longer body dimension from the center of the wake, and the streamwise vortical tails extend downstream from one of the hemispherical ends. Incidentally, the calculated drag coefficient was 0.70, within 0.5% of the value for a true sphere.

The solution at Re=250 was used as an initial condition for a computation at Re=300. An unsteady wake quickly evolved with the same orientation. However, this orientation was unstable, and a slow rotation through 90° followed. The wake eventually adopted a preferred orientation aligned with the minor axis of the body, which was reached after approximately 1000 time units and 130 oscillation periods.

The axisymmetry of a perfect sphere means that there is no preference to the orientation of the wakes produced at the Reynolds numbers employed here. Interestingly, the addition of an asymmetry to the body shows that there are distinct preferences of orientation for the steady and unsteady wakes.

The isosurface plots in Fig. 5 show that the wake maintains the familiar hairpin shedding pattern observed behind a sphere,[7,9,22] and that planar symmetry is maintained at Re=300.

Mittal[8] observed that for a sphere, the unsteady wake loses its planar symmetry somewhere in the range of $350 \lesssim \mathrm{Re} \lesssim 375$. The axisymmetry of the body poses a challenge for the investigation of the breakdown of planar symmetry, as there is no preferential orientation of the symmetric wake. Here the nearly spherical cylinder with LR=1.04 is computed at Reynolds numbers up to Re=370, and the axial force coefficient is monitored. This force component is zero for planar-symmetric wakes. Figure 6 shows traces of the transverse forces acting on the body at Re=350 and 360. At Re=350 the plot demonstrates planar-symmetric properties, with the variation in transverse force occurring almost solely on a horizontal plane. At Re=360, the behavior is very different, with no preferential wake orientation being detected.

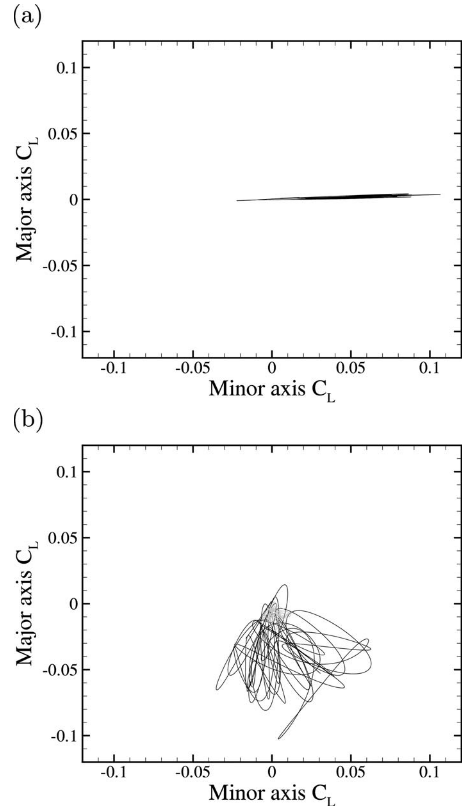

FIG. 6. Traces of the transverse force coefficients ($C_F = F/\frac{1}{2}\rho A U^2$, where F is the force, ρ is the fluid density, and A is the projected frontal area of the body) in a plane normal to the direction of flow for a cylinder with LR=1.04. Reynolds numbers (a) Re=350 and (b) 360 are shown. Data were acquired over approximately 300 time units.

Loss of planar symmetry resulted in evolution of nonzero mean and fluctuating components of side force along the major axis of the cylinder. Figure 7 plots these quantities at a number of Reynolds numbers through the transition. Scatter in the data beyond Re=350 is a result of the relatively short sample sets obtained due to the expense of the computations. However, it is clear that planar symmetry appears to evolve through a continuous (or supercritical)

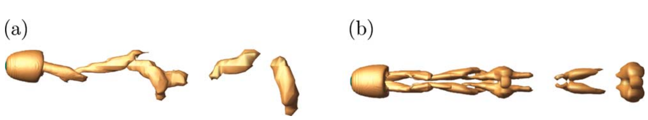

FIG. 5. (Color online) Rotation of the unsteady wake computed at Re=300, from (a) the initial orientation to emerge from the steady-state solution at Re=250 to (b) the preferred orientation reached after approximately 1000 time units, and 130 periods. Isosurfaces and flow direction are as per Fig. 3.

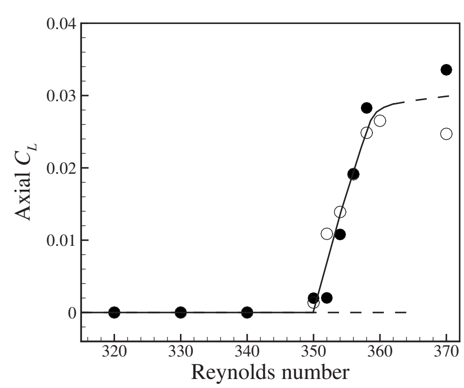

FIG. 7. Reynolds number dependence of the mean (solid symbols) and standard deviation (open symbols) of the axial force coefficient time history for a cylinder with LR=1.04. Solid and dashed lines are added for guidance and trace the planar-symmetric and asymmetric mode branches through a supercritical transition at Re≈350.

bifurcation[9,10] at $Re=350\pm2$, a substantial refinement of the previously reported Reynolds number range for this transition.

This work was supported by the Australian Research Council Discovery Grant No. DP0555897. Computations were performed on the Australian Partnership for Advanced Computing (APAC) National Facility.

[1]M. Provansal, C. Mathis, and L. Boyer, "Bénard-von Kármán instability: Transient and forced regimes," J. Fluid Mech. **182**, 1 (1987).
[2]C. H. K. Williamson, "Vortex dynamics in the cylinder wake," Annu. Rev. Fluid Mech. **28**, 477 (1996).
[3]B. Ghidersa and J. Dušek, "Breaking of axisymmetry and onset of unsteadiness in the wake of a sphere," J. Fluid Mech. **423**, 33 (2000).
[4]C. H. K. Williamson, "The existence of two stages in the transition to three-dimensionality of a cylinder wake," Phys. Fluids **31**, 3165 (1988).
[5]D. Barkley and R. D. Henderson, "Three-dimensional Floquet stability analysis of the wake of a circular cylinder," J. Fluid Mech. **322**, 215 (1996).
[6]T. A. Johnson and V. C. Patel, "Flow past a sphere up to a Reynolds number of 300," J. Fluid Mech. **378**, 19 (1999).
[7]A. G. Tomboulides and S. A. Orszag, "Numerical investigation of transitional and weak turbulent flow past a sphere," J. Fluid Mech. **416**, 45 (2000).
[8]R. Mittal, "A Fourier-Chebyshev spectral collocation method for simulating flow past spheres and spheroids," Int. J. Numer. Methods Fluids **30**, 921 (1999).
[9]G. J. Sheard, M. C. Thompson, and K. Hourigan, "From spheres to circular cylinders: Non-axisymmetric transitions in the flow past rings," J. Fluid Mech. **506**, 45 (2004).
[10]G. J. Sheard, M. C. Thompson, and K. Hourigan, "Asymmetric structure and non-linear transition behaviour of the wakes of toroidal bodies," Eur. J. Mech. B/Fluids **23**, 167 (2004).
[11]D. R. Monson, "The effect of transverse curvature on the drag and vortex shedding of elongated bluff-bodies at low Reynolds-number," J. Fluids Eng. **105**, 308 (1983).
[12]T. Leweke and M. Provansal, "The flow behind rings: Bluff body wakes without end effects," J. Fluid Mech. **288**, 265 (1995).
[13]G. J. Sheard, M. C. Thompson, and K. Hourigan, "From spheres to circular cylinders: The stability and flow structures of bluff ring wakes," J. Fluid Mech. **492**, 147 (2003).
[14]G. J. Sheard, M. C. Thompson, K. Hourigan, and T. Leweke, "The evolution of a subharmonic mode in a vortex street," J. Fluid Mech. **534**, 23 (2005).
[15]N. W. M. Ko, C. W. Law, and K. W. Lo, "Mutual interference on transition of wake of circular cylinder," Phys. Fluids **16**, 3138 (2004).
[16]C. H. K. Williamson, "Oblique and parallel mode of vortex shedding in the wake of a circular cylinder at low Reynolds numbers," J. Fluid Mech. **206**, 579 (1989).
[17]C. Norberg, "An experimental investigation of the flow around a circular cylinder: Influence of aspect ratio," J. Fluid Mech. **258**, 287 (1994).
[18]L. Schouveiler and M. Provansal, "Periodic wakes of low aspect ratio cylinders with free hemispherical ends," J. Fluids Struct. **14**, 565 (2001).
[19]M. Provansal, L. Schouveiler, and T. Leweke, "From the double vortex street behind a cylinder to the wake of a sphere," Eur. J. Mech. B/Fluids **23**, 65 (2004).
[20]H. M. Blackburn and S. J. Sherwin, "Formulation of a Galerkin spectral element-Fourier method for three-dimensional incompressible flow in cylindrical geometries," J. Comput. Phys. **197**, 759 (2004).
[21]J. Jeong and F. Hussain, "On the identification of a vortex," J. Fluid Mech. **285**, 69 (1995).
[22]R. Mittal, "Planar symmetry in the unsteady wake of a sphere," AIAA J. **37**, 388 (1999).